

Chapter 4

H I in intermediate redshift groups

In this chapter, we present the results of the GMRT H I observation of two groups at an intermediate redshift of $z \sim 0.06$. Both our sources belong to a bigger sample of 25 optically selected groups at an intermediate redshift of 0.06. The larger scientific aim of this project is to study the cold gas and hot gas evolution of galaxies in groups at this redshift. Here, we discuss the H I observations carried out so far, the H I contents of the galaxies and their H I deficiencies.

4.1 Introduction

Cluster environments have been studied intensively through various observations over the last three decades. Environment plays a very important role in the evolution of galaxies in the cluster. Through galactic collisions or interaction with the hot, dense intra-cluster medium (ICM), galaxies evolve in clusters. The timescales of galaxy evolution in clusters is also relatively short. Significant evolution in the morphologies, gas content and star formation of disk galaxies have been seen in this environment between $z \sim 0.2 - 0.3$ and $z \sim 0$. Spiral galaxies have been seen to be a factor of 2–3 more abundant at $z \sim 0.5$ than at the present epoch, while S0 galaxies are proportionally less abundant in distant clusters [42]. This suggests a large number of lenticulars (S0) we see at the present epoch have basically evolved from the spirals observed at $z \sim 0.5$.

Groups of galaxies are believed to contain the bulk of the matter in the Universe ([47]). They are the characteristic structures formed at the present epoch through hierarchical merging, and thus an understanding of the formation of galaxies and of the large-scale structure of the Universe requires an understanding of galaxy groups. The low velocity dispersion of galaxies in groups encourages tidal interaction, and results in an enhanced occurrence of strong encounters, accretion and mergers. Hence, not only are groups the most common environment for galaxies, but they also provide an environment which is conducive to a rapid change in galaxy properties. Given the crucial role they play, galaxy groups have not received the intensive study they deserve.

However, recent studies are revealing that galaxies evolve in group environments too. Relatively recent X-ray observations of the intra-group medium (IGM) of several groups indicate the metallicity to vary from 0.1 to 0.6 solar metallicity [95]. Another observation states the average metallicity of the IGM of a set of groups to be 0.3 [18]. Since stars can be the only source of these metals, it is obvious that part of this gas is contributed by the group members, indicating that clusters are not the only environment where galaxies lose gas and

evolve. Galaxies in groups, like the ones in clusters, have been found to be deficient (a term used to measure gas loss of a galaxy compared to a field galaxy of same size and similar morphological type) in neutral hydrogen ($H I$). They can lose gas either through gravitational interactions with other members in the group or be stripped by the intra-group medium (IGM). Studies have revealed deficiency of neutral hydrogen in galaxies belonging to compact groups ([155], [136]) and loose groups ([102], [125]).

The following work is an $H I$ study of two optically selected groups at a redshift of 0.06. These two optically selected groups form a part of a bigger unbiased, statistical sample of about 25 groups, which have been chosen for a multi-wavelength survey. The primary aim of the project is to understand the nature and evolution of the galaxies in groups at an intermediate redshift, and the role played by cold gas (radio) and hot gas (X-ray) in their history.

4.2 GMRT observations

4.2.1 Source Selection

In 2003, the XMM-IMACS project was launched to take advantage of the advent of large-scale redshift surveys, and the simultaneous availability of sensitive X-ray telescopes and large ground-based facilities. An unbiased sample of 25 groups were selected for a multi-wavelength study. The optical observations for this sample are being done using the IMACS multi-object camera and spectrograph [12], recently installed on the 6.5 m Baade/Magellan telescope at Las Campanas. The X-ray observations are being done using the XMM-Newton X-ray observatory, the most sensitive X-ray telescope launched to date.

The sample of groups was chosen from the catalogue of 2209 groups derived by Merchan & Zandivarez (2002)[89] from the first data release of the 2dF galaxy redshift survey [31]. The constraints placed were the following

- Redshift $z=0.060-0.063$ At this redshift, the typical virial radius of groups, ~ 1 Mpc,

corresponds to 13' ideally matched to both the XMM and IMACS fields of view.

- Velocity dispersion $\sigma < 500 \text{ km s}^{-1}$, Richness $N_{\text{gal}} \geq 5$ This limits the study to poor and sluggish systems, which typify the environment of over $\sim 50\%$ of all galaxies and is conducive to rapid dynamical evolution [91].

Of the groups that satisfied these criteria, 25 were selected entirely at random. No further constraints of regularity, optical luminosity or dynamical status were applied. Hence the sample contains groups spanning a wide range of properties, subject to having an overdensity which distinguishes them in the friends-of-friends analysis.

Two groups, MZ5383 and MZ9014, from this sample have been observed in H I 21 cm line using the Giant Metrewave Radio Telescope near Pune in India. IMACS has a field of view (30') perfectly matched to that of XMM and almost matched to the primary beam of GMRT (24') at 21 cm. This allows the entire group, at a redshift of 0.06, to be imaged and studied in a single pointing. The sources MZ5383 and MZ9014, both observed by the XMM, were chosen to study the effect of the hot gas on the cold gas in the galaxies. MZ5383 has not been detected with any IGM emission and the 3σ upper limit to the diffuse 0.3–2 keV luminosity is $< 3.3 \times 10^{41} \text{ erg/s}$ [114]. The expected luminosity of this group from the $L_X - \sigma_V$ relation of [104] was $\sim 4 \times 10^{42} \text{ erg/s}$. MZ9014 is relatively X-ray rich, with a velocity dispersion of 236 km s^{-1} and X-ray luminosity $\sim 6 \times 10^{40}$ [114]. Relevant details of the sources are listed in table 1.

4.2.2 H I Observation

The two sources mentioned above were observed in H I 21cm line with the GMRT. This is an interferometric array of 30 antennas, each of 45m in diameter, spread over distances upto 25 km. The system temperature, gain (K/Jy) and full width at half maximum of the primary beam of the instrument in 1420 MHz are 76K, 0.22 and 24' respectively. Data obtained with the GMRT were reduced using AIPS (Astronomical Image Processing System). The following procedure was used to get the final H I cubes. Bad data (dead antennas, antennas with

Table 4.1: Source and Observation Specifications

Group	Pointing centre (J2000)	σ kms ⁻¹	L_x erg/s	G_n	τ (hrs)	$\Delta\nu$ (MHz)	rms (mJy)
MZ5383	12 34 58.8 -03 37 11.9	437	$<3.3 \times 10^{41}$	19	13	16	0.25
MZ9014	00 37 44.3 -27 30 35.1	236	6×10^{40}	23	21	16	0.37

note to table 1. σ represents the velocity dispersion, L_x is the IGM X-ray luminosity, G_n is the membership of the groups. τ in hours in the integration time. $\Delta\nu$ in MHz is the baseband bandwidth used for the GMRT observation. 'rms' in mJy, is the per channel rms achieved in the analysis of the data.

significantly lower gain than others, RFI) were flagged and the data was calibrated for amplitude and phase using standard primary and secondary calibrators. The spectral responses of the filters were corrected by calibrating the data using a standard primary calibrator or when available a strong secondary calibrator. The calibrated data were continuum subtracted using AIPS tasks 'UVSUB' (used to subtract a model, in this case the clean image, from the UV data) and 'UVLIN' (used to subtract continuum by making linear fits to the UV data). The task 'IMAGR' was then used to get the final 3 dimensional H I data cubes. Details of the observation are listed in table 1.

4.3 Results

Out of 13 spirals, only one galaxy in MZ5383 was detected to have H I , and two others showed marginal signs of H I detections. There were no detections from the rest of the galaxies. In MZ9014 none of the 13 spiral galaxies were detected with H I . The H I content of spiral galaxies depends both on their sizes and morphological types. In fact, the disk size seems to be a more important diagnostic for the H I mass than the morphological type [59]. The expected H I content of the individual spirals in the two groups were estimated. This is basically the H I mass expected in a field spiral galaxy of similar morphological type [59] and size. Table 2 lists the H I surface density values ($M_{H I}/D_f^2$) observed in field spirals of

Table 4.2: Expected surface matter densities for different morphological types (adapted from [59] for using RC3 diameters instead of UGC diameters.

Morphological type (<i>M.T.</i>) & Index	$\log(\frac{M_{H_I}/D_l^2}{M_\odot/kpc^2})_{pred} \pm \text{s.d}$
Elliptical,S0,S0/a	1 6.69 ± 0.27
Sa,Sab	2 6.77 ± 0.32
Sb	3 6.91 ± 0.26
Sbc	4 6.93 ± 0.19
Sc	5 6.87 ± 0.19
Scd,Sd,Irr,Sm,Sdm, dSp	6 6.95 ± 0.17
Pec	7 7.14 ± 0.28

different morphological types.

The parameter that measures whether a galaxy has an excess or a lower H I content compared to a field sample is known as H I deficiency and is defined as [59],

$$\text{def}_{H_I} = \log \frac{M_{H_I}}{D_l^2}|_{field} - \log \frac{M_{H_I}}{D_l^2}|_{obs} \quad (4.1)$$

where M_{H_I} is the H I mass of a galaxy and D_l is the optical major isophotal diameter (in kpc) measured at or reduced to a surface brightness level $m_B = 25.0$ B-m/ss. The expected values of M_{H_I}/D_l^2 for various morphological types are taken from [59]. While [59] used the UGC blue major diameters, we have used the RC3 major diameters. To take care of the difference in the surface matter densities that result from the use of RC3 diameters, we add a value of 0.08 [51] to the expected surface matter densities given by [59].

The values of D_l are derived from the angular major diameters from the optical observations carried out on these two groups. A hubble constant of $75 \text{ km s}^{-1} \text{ Mpc}^{-1}$ has been used to get the distances to the groups from their average optical velocities, obtained from the optical observations. The distance to both the groups is $\sim 250 \text{ Mpc}$. In absence of detailed morphological classification of the spirals in these groups, the expected M_{H_I}/D_l^2 of Sb type has been used for all of them. Table 3. and 4. lists the spiral galaxies in the groups MZ5383 and MZ9014 (observed by the GMRT), their co-ordinates, their angular major diameters, redshift values from optical observations (IMACS data), optical velocities (V_{opt}) (both from

the IMACS optical data and NED), expected H I content and upper limit of H I mass estimated from the GMRT observations.

The detection in the group MZ5383 is of a spiral at the position 12 35 08.66 -03 35 19.32 (referred hereafter as galaxy A). Fig.1 shows the total H I map of this galaxy. By definition the total H I maps are the integrated flux density maps,

$$I_{tot}(\alpha, \delta) = \Delta v \sum_{i=1}^{N_{chan}} S_v(\alpha, \delta, \nu_i) \quad (4.2)$$

Here $S_v(\alpha, \delta, \nu_i)$ is the observed flux density at the position (α, δ) in channel i (which has frequency ν_i) and N_{chan} is the total number of channels over which the H I line exists. The total H I maps were produced at an angular resolution $25''$, which translates to a physical length of 30kpc at the distance to the galaxy. The spectrum taken along the direction of the galaxy is presented in figure 2. The spectrum was fitted with a second order polynomial and the baseline was removed. The integrated flux density was converted to H I mass using the following equation,

$$M_{H_I}(M_{\odot}) = 2.36 \times 10^5 D^2 \Delta v \sum_{i=1}^{N_{chan}} S_i \quad (4.3)$$

where D is the distance to the galaxy. The H I mass in this galaxy was found to be $\sim 4.7 \times 10^9 M_{\odot}$. The channel map for this galaxy, at a velocity resolution of ~ 60 km/s, is displayed in Fig 3.

The two other galaxies in MZ5383, where H I detection were a possibility are at positions 12 35 10.72 -03 37 36.48 (galaxy B) and 12 34 38.71 -03 41 22.92 (galaxy C). In both the cases the expected H I mass in the galaxy was higher than the sensitivity limits of this observation (table 3). The channel maps overlaid on the optical images and the spectra towards these galaxies are presented in figures 4 to 7. A comparison of the spectra from these above three galaxies with noise is shown in figure 8. The three solid lines in red represent these three galaxies (A, B and C) and the broken blue lines represent the noise along positions where there are no known sources in the group MZ5383. While galaxy A was

an unambiguous H I detection, galaxies B and C were doubtful cases of detection. However, they were considered non-detections, after the spectra from the two different polarization outputs did not reproduce the similar spectra.

In the absence of H I detection in individual galaxies, co-adding of the H I spectra were carried out for MZ9014 and for all the galaxies except the one detected in MZ5383. In this method, the expected line centre in the spectra from the spirals were shifted to zero kms^{-1} , and then the spectra were added to improve the signal to noise ratio. In this case, however, co-adding the spectra did not result in any significant improvement, the reason probably being very few numbers of galaxies. The upper limits to the H I masses of all the spirals were estimated using a flux value of three times the per channel map rms and a velocity width of 150 km/s, using the equation 3. These values along with their expected H I masses are listed in tables 3 and 4. To establish H I deficiency in single galaxies in these groups is difficult because of the scatter in the field surface density values. But on an average we see a trend towards lesser gas content in most of these galaxies. Also the galaxy where we see the presence of H I belongs to the group with lower X-ray luminosity.

4.4 Discussion

This work is a part of an on-going project about the study of galaxy evolution in group environment at an intermediate redshift of 0.06. With a sample of an unbiased selection of 25 groups and X-ray, optical and radio data on them, the long term scientific aim of this project is to understand the neutral gas evolution and stripping in this environment, the relation between the H I deficiency and the X-ray emitting IGM of the groups, the relation of cold gas with general group properties like the IGM temperature, luminosity or the dynamical state of the group.

In the local universe recent studies have revealed the importance of IGM assisted stripping processes in group environment, especially the groups which have a hot IGM [39], [78], [113], [126]. Because of low dispersion and low IGM density, ram pressure stripping was

Table 4.3: MZ5383: Expected and Observed H I content

Coordinate J2000	M-type	d_l ($^{\circ}$)	z (IMACS)	V_{opt} (IMACS) (kms^{-1})	V_{opt} (NED) (kms^{-1})	expected H I mass (M_{\odot})	detected H I mass (M_{\odot})
12 35 08.66 -03 35 19.32	S	0.55	0.06135	18405	18531	$1.3\text{E}+10$	$4.71\text{E}09$
Coordinate J2000	M-type	d_l ($^{\circ}$)	z (IMACS)	V_{opt} (IMACS) (kms^{-1})	V_{opt} (NED) (kms^{-1})	expected H I mass (M_{\odot})	upper limit on H I mass (M_{\odot})
12 35 10.72 -03 37 36.48	S	0.25	0.06152	18456	18543	$2.6\text{E}+09$	$1.6\text{E}+09$
12 34 56.28 -03 40 54.12	S	0.22	0.05950	17850	17877	$2.1\text{E}+09$	$1.6\text{E}+09$
12 34 45.88 -03 34 13.44	S	0.25	(0.0626)	-	18767	$2.6\text{E}+09$	$1.6\text{E}+09$
12 35 03.62 -03 40 28.56	U	0.18	0.06169	18507	18677	$1.4\text{E}+09$	$1.6\text{E}+09$
12 34 38.71 -03 42 21.60	S	0.18	0.06202	18606	18587	$1.4\text{E}+09$	$1.6\text{E}+09$
12 34 38.71 -03 41 22.92	U	0.43	0.0617	18510	18483	$8.0\text{E}+09$	$1.6\text{E}+09$
12 35 10.79 -03 35 11.04	U	0.11	0.0587	17610	-	$5.3\text{E}+08$	$1.6\text{E}+09$
12 34 42.56 -03 29 04.56	U	0.11	(0.0595)	-	17838	$5.5\text{E}+08$	$1.6\text{E}+09$
12 35 14.06 -03 29 56.04	U	-	0.0589	17670	-	-	$1.6\text{E}+09$
12 35 12.70 -03 31 00.12	U	0.15	0.0596	17880	-	$9.5\text{E}+08$	$1.6\text{E}+09$
12 34 41.38 -03 33 00.00	U	0.12	(0.0602)	-	18048	$6.3\text{E}+08$	$1.6\text{E}+09$
12 35 20.87 -03 36 18.00	U	-	0.0621	18630	-	-	$1.6\text{E}+09$
12 35 02.80 -03 40 43.32	E	0.51	0.06167	18501	18559	-	-
12 35 09.06 -03 35 49.56	E	0.43	0.059283	17784	17876	-	-
12 34 18.62 -03 34 50.88	S*	0.24	(0.0571)	-	17137	-	-
12 34 19.16 -03 34 41.16	U*	0.15	(0.0572)	-	17148	-	-
12 34 16.21 -03 33 47.52	Irr**	0.18	(0.0598)	-	17928	-	-
12 35 11.47 -03 28 49.80	E	0.22	0.0601	18030	18250	-	-

Table 4.4: MZ9014: Expected and Observed H I content

Coordinate J2000	M-type	d_l ($^{\circ}$)	z (IMACS)	V_{opt} (IMACS) (kms^{-1})	V_{opt} (NED) (kms^{-1})	expected H I mass (M_{\odot})	upper limit on H I mass (M_{\odot})
00 38 06.09 -27 30 26.64	S	0.22	0.05959	17877	17916	2.1E+09	2.4E+09
00 37 37.10 -27 30 52.92	S	-	0.06123	18369	18462	-	2.4E+09
00 38 09.38 -27 33 27.36	S	0.16	0.06101	18303	18548	1.1E+09	2.4E+09
00 37 45.09 -27 31 04.08	Irr	0.13	0.0612	18360	18491	7.6E+08	2.4E+09
00 37 21.91 -27 30 13.68	S	0.11	0.06083	18249	-	5.4E+08	2.4E+09
00 38 03.74 -27 30 40.32	S	-	0.0613	18390	-	2.4E+09	2.4E+09
00 38 12.38 -27 32 36.24	S	0.38	0.06089	18267	18222	6.3E+09	2.4E+09
00 37 43.51 -27 31 54.12	Irr	0.14	0.06202	18606	-	8.4E+08	2.4E+09
00 37 37.10 -27 30 54.00	U	0.22	(0.0611)	-	18317	2.1E+09	2.4E+09
00 38 01.99 -27 32 02.04	U	0.20	0.06027	18081	-	1.7E+09	2.4E+09
00 37 03.41 -27 34 48.36	U	-	0.0606	18180	-	2.4E+09	2.4E+09
00 37 13.42 -27 29 20.76	U	-	0.06010	18030	-	2.4E+09	2.4E+09
00 38 19.03 -27 33 00.40	Irr	0.22	0.06106	18318	18459	2.1E+09	2.4E+09
00 37 25.10 -27 31 58.8	S0	0.22	0.06008	18024	18257	-	-
00 36 53.47 -27 34 26.1	S*	-	0.06078	18234	-	-	-
00 38 25.20 -27 25 15.0	E	0.19	0.05941	17823	17808	-	-
00 38 05.50 -27 29 30.0	S0	0.16	0.06006	18018	18257	-	-
00 37 39.40 -27 27 59.0	E	0.51	0.06099	18297	18429	-	-
00 37 19.80 -27 23 40.20	E	0.23	(0.0630)	-	18887	-	-
00 37 01.87 -27 32 58.56	E	-	0.06175	18525	-	-	-
00 37 07.84 -27 29 31.92	E	-	0.06187	18561	-	-	-
00 36 51.94 -27 30 23.04	U*	-	0.05959	17877	18077	-	-
00 36 49.30 -27 27 54.72	U*	-	(0.0605)	-	18135	-	-

Notes to tables 3 and 4: Each table has been divided into parts by a horizontal line through the table. Galaxies above the horizontal line in the tables are expected to be detected in H I, galaxies below the line are not expected to be detected in H I as they are either early types (E or S0) or they are towards the edge of the FWHM of the GMRT primary beam (marked by '*' in the second column). In column two 'U' and 'Irr' implies unknown morphological type and irregulars, however, they have all been considered in the spiral category for this work. In column four, in cases where redshift measurements are not available from the IMACS data, redshift values from NED have been quoted within brackets. A '-' in the sixth column implies absence of radial velocity values in NED.

not considered a favoured gas removal mechanism in groups. However, recent studies of groups which possess a hot IGM like in clusters, show ram pressure can remove substantial gas from the galaxies in these groups. The current work, is an attempt to extend this study of the H I content of galaxies in X-ray bright groups, to intermediate redshifts ~ 0.06 , as galaxies are known to evolve in redshift as well.

MZ5383 is a loose group with 19 members, of which 16 are spiral galaxies. Of these 16 spirals, 13 were observed with the GMRT. Only one, at position RA: 12 35 08.66 dec: -03 35 19.32 (galaxy A), was detected in H I. The 3σ mass limit achieved for the H I non detected galaxies in this group was $\sim 1.6 \times 10^9 M_{\odot}$. The galaxy detected in H I is the biggest spiral of the group. The major diameter of this galaxy is $0.6'$ which is ~ 43 kpc at the distance to the galaxy. The expected H I mass of this galaxy was $\sim 1.3 \times 10^{10} M_{\odot}$, whereas the observed mass is $\sim 4.7 \times 10^9 M_{\odot}$.

The $\log(M_{\text{HI}}/D_i^2)$ for this galaxy is 6.47, whereas for a field spiral of this size it should be $\sim 6.91 \pm 0.26$ [59]. This indicates that this galaxy is moderately deficient in H I. The reason for this H I deficiency can probably be found in the total H I map presented in figure 1. The H I disk of this galaxy looks disturbed, with most of the gas being present outside the galaxy. The H I disk is stretched to the south, towards an elliptical galaxy, which is also a member of this group. This elliptical galaxy is within $0.5'$ from the spiral, at position 12 35 09.1 -03 35 50 and velocity 17876 km/s. In the channel map (fig. 3), the stretched mass of H I is seen to be shifted towards this elliptical in the south. Hence it is possible for them to undergo a tidal interaction and remove gas from the spiral.

Apart from just one galaxy, none of the galaxies in either groups were detected in H I. Out of the 13 spirals in MZ5383, 6 more detections could have been possible if all of them had the amount of gas expected in galaxies of their size. The expected H I masses in them were higher than the upper limits of H I mass achieved from this observation. Similarly, in MZ9014, 13 spirals were observed with GMRT and about 4 of them could have been detected had they contained their expected amount of H I. The 3σ detectable mass limit achieved in this group is $2.4 \times 10^9 M_{\odot}$. The non detection of 10 spirals, from both the groups, indicate

gas deficiency in these groups. Also the sole detection belongs to an X-ray poor group. Due to the large scatter in the H I surface densities of the field spirals (table 2), is difficult to conclusively say if a single galaxy is H I deficient compared to the field sample. However, in this case, the bias of all the H I detectable galaxies towards a lower than normal gas content, suggests H I deficiency in these spirals rather than this being the effect of the scatter in the field values. With only 2 groups studied so far, it is difficult to establish whether in general X-ray bright groups will be more H I deficient than non X-ray bright groups at the this redshift. Further observations of more groups in our sample, will help us to know, whether we find a systematic H I deficiency in X-ray bright groups compared to non X-ray bright groups, and if the deficiency is related to the hot IGM of the groups. We have been granted 36 hrs in GMRT, on one more group out of the remaining 23 groups. Observations are due in Aug, 2007.

4.5 Conclusion

This work is a part of an on-going project: a multiwavelength study of an unbiased sample of 25 groups, to study the cold gas and hot gas evolution of galaxies in groups at an intermediate redshift. However, this chapter focuses on the GMRT H I study of 2 of the 25 groups. The main outcome of the H I observations of these groups are the following;

- One galaxy in MZ5383, a group at $z \sim 0.06$ and with an X-ray poor IGM, has been detected in H I .
- The galaxy is found to be H I deficient, and H I image of this galaxy suggests an interaction with a neighboring large elliptical galaxy to be the cause of the gas loss.
- On an average the galaxies tend to be H I deficient. No galaxy was detected in the group which was brighter in X-rays. More data is required to statistically check if the H I deficiency is related to the hot IGM.

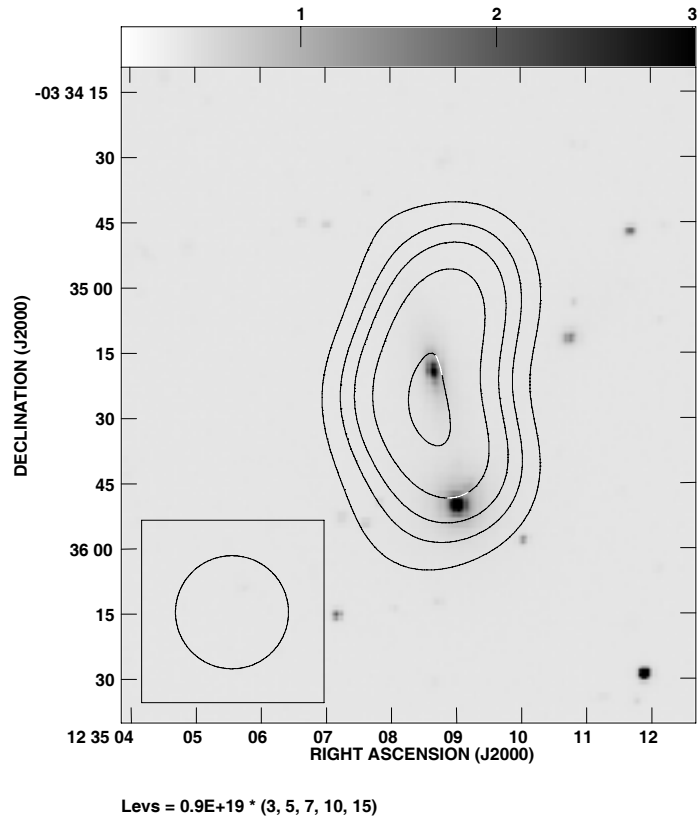


Figure 4.1: Total H I map of the galaxy at position 12 35 08.66 -03 35 19.32 in MZ5383 group overlaid on the optical image: HI column density contours levels= $2.3E+19 /\text{cm}^2 \times 3,5,7,9,11$

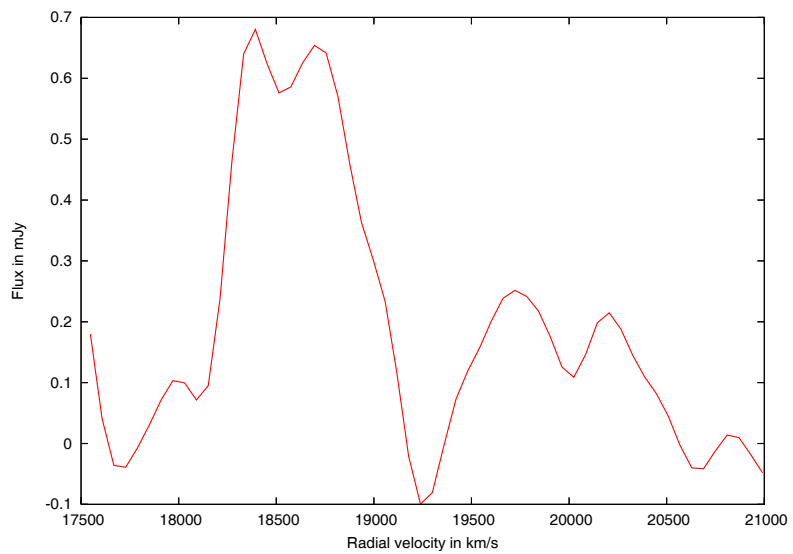
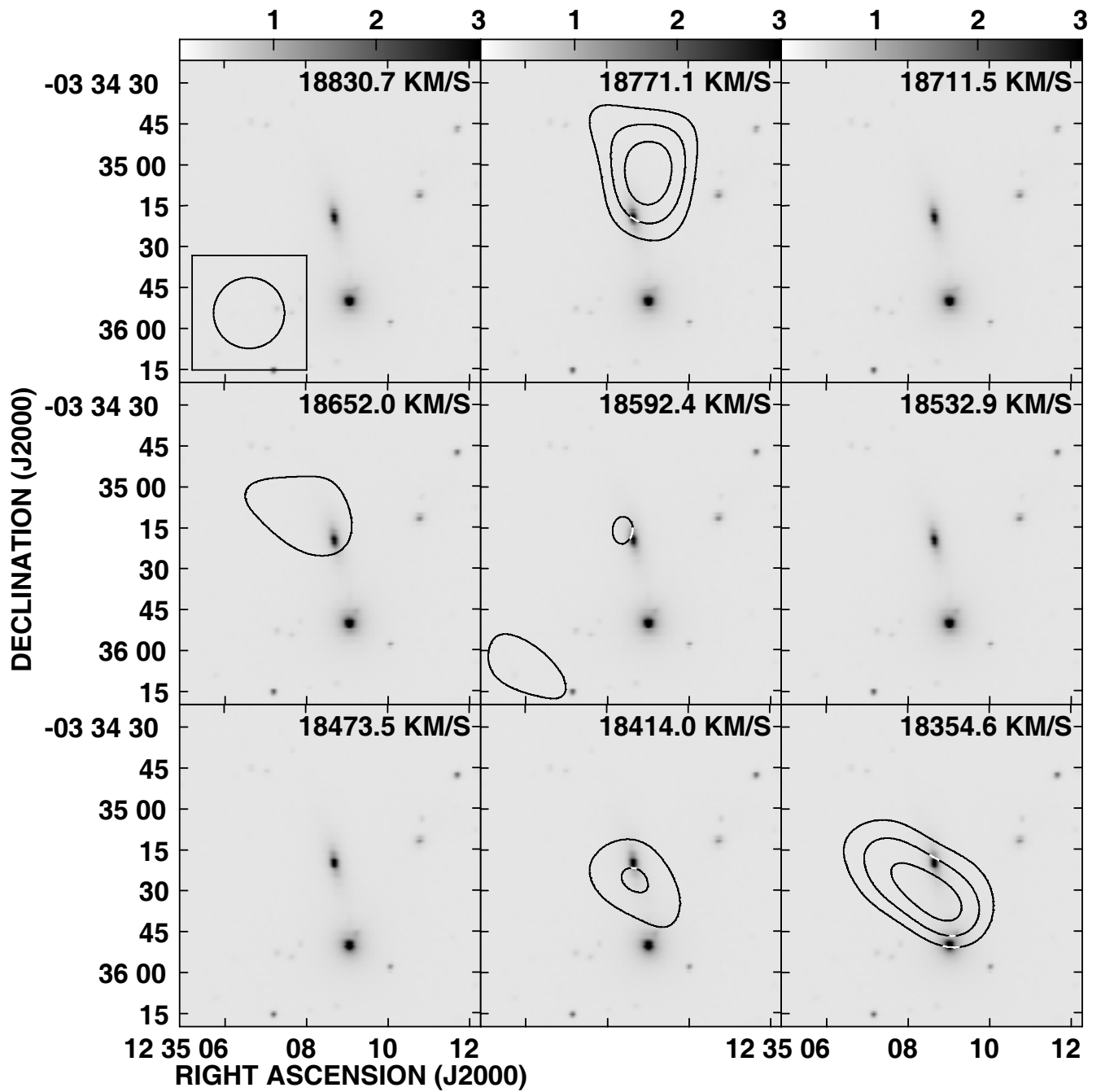


Figure 4.2: H I spectra of the galaxy at position 12 35 08.66 -03 35 19.32 in MZ5383 group, optical velocity of the galaxy is 18405 km s^{-1}



Cont peak flux = $8.2561\text{E-}04$ JY/BEAM
 Levs = $1.200\text{E-}04 * (3, 4, 5)$

Figure 4.3: H I channel maps of the galaxy at position 12 35 08.66 -03 35 19.32 in MZ5383 group overlaid on the optical image

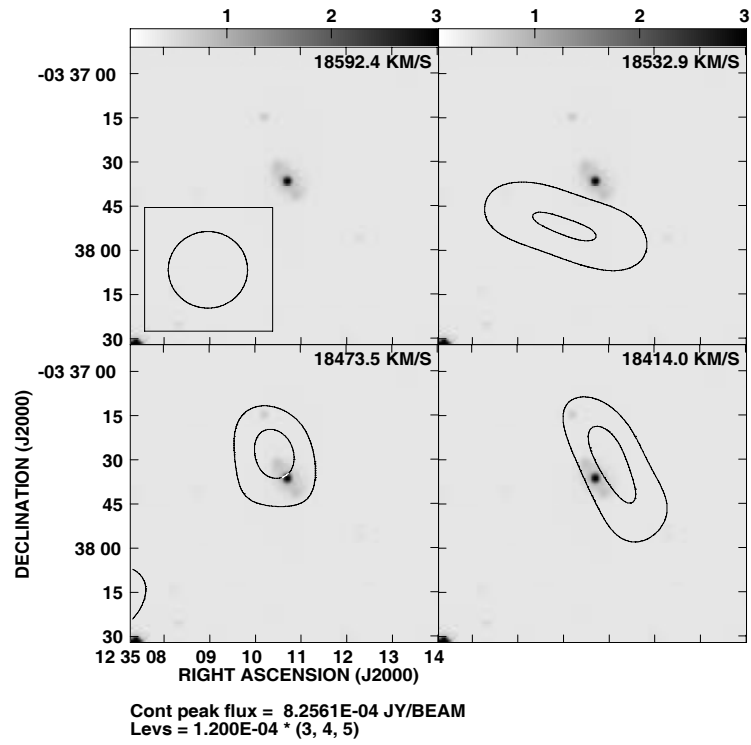


Figure 4.4: Channel maps of galaxy at position 12 35 10.72 -03 37 36.48

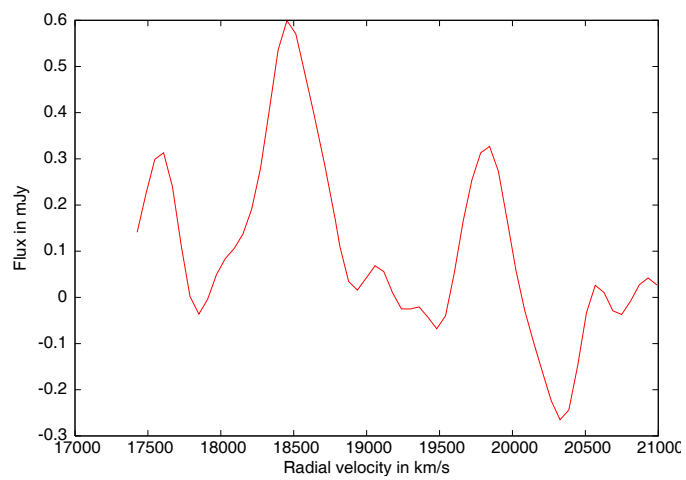


Figure 4.5: H I spectra of the galaxy at position 12 35 10.72 -03 37 36.48, optical velocity of this galaxy is 18456 km s^{-1}

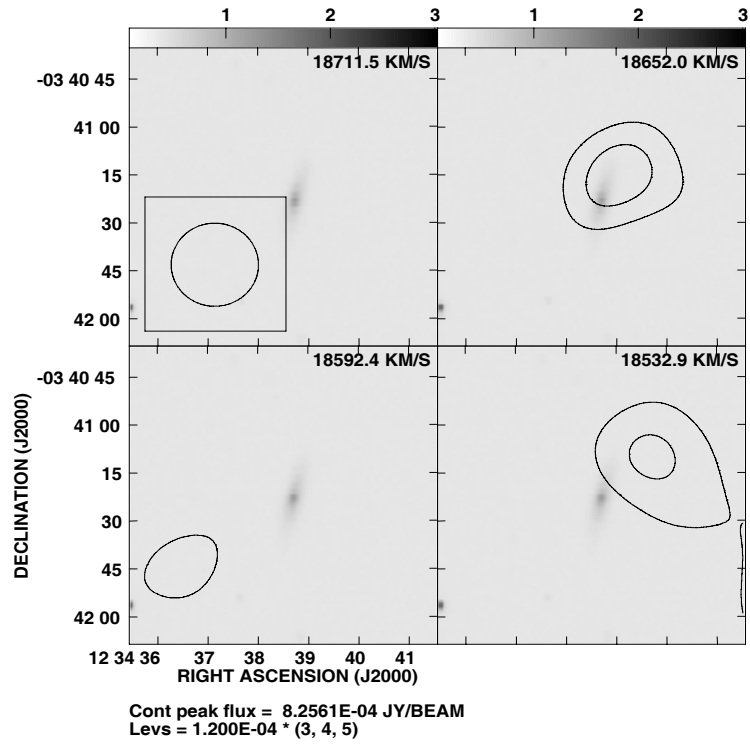


Figure 4.6: Channel maps of galaxy at position 12 34 38.71 -03 41 22.92

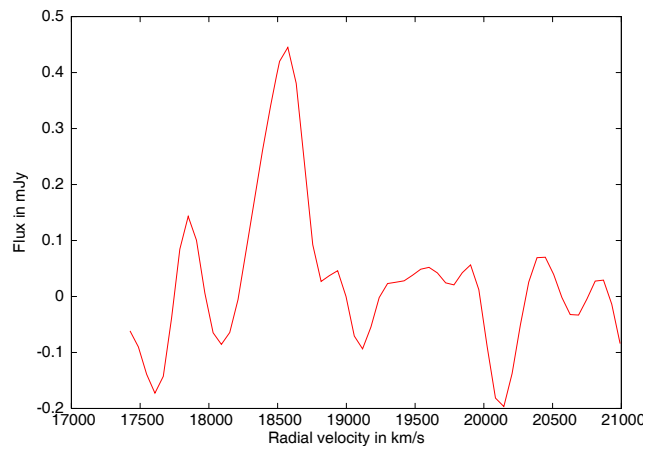


Figure 4.7: H I spectra of the galaxy at position 12 34 38.71 -03 41 22.92, optical velocity of this galaxy is 18510 km s^{-1}

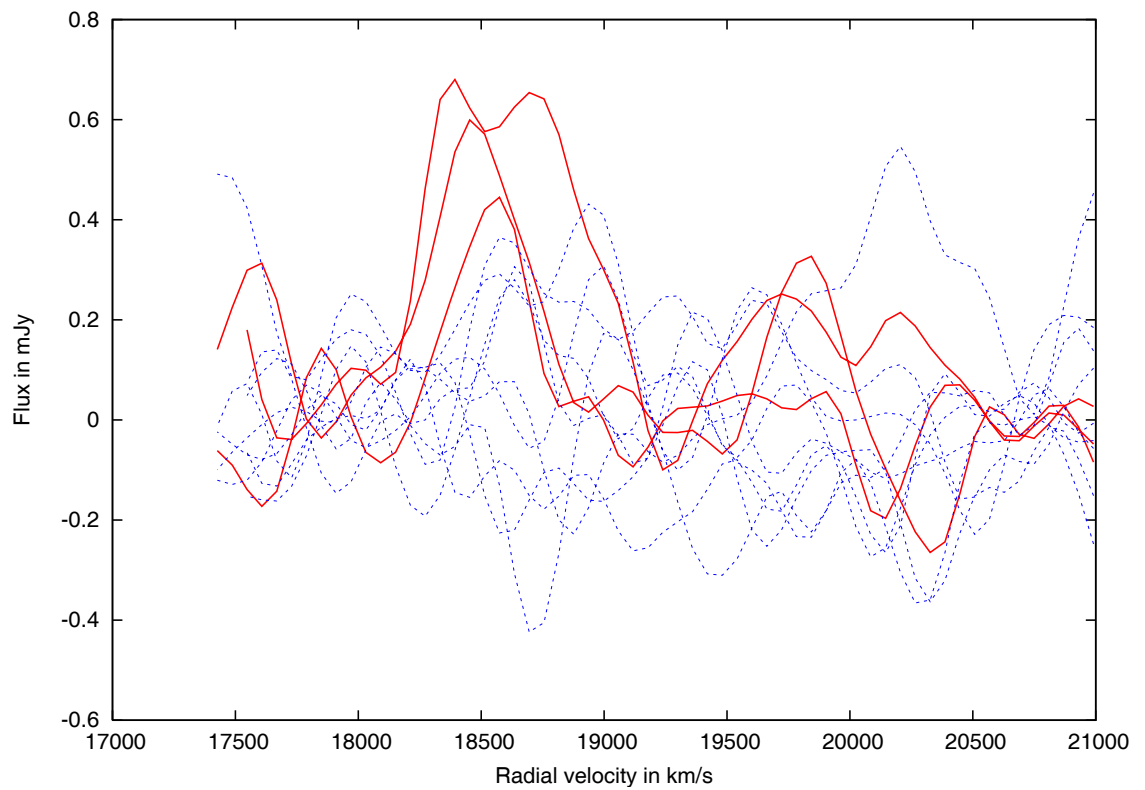


Figure 4.8: H I spectra of the galaxies A, B and C (discussed in text) plotted along with noise from positions where no known source were present. The 3 red solid lines denote the 3 galaxies.

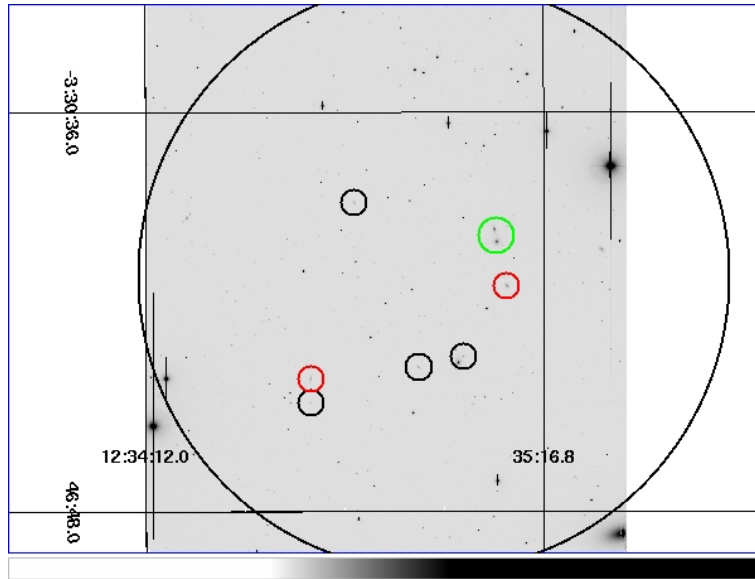


Figure 4.9: The optical image of the group MZ5383. The circle with the largest diameter denotes the GMRT primary beam (FWHM). The small green circle denotes the H I detected galaxy in this field. All the galaxies which could have been detected if they were not H I deficient are marked in either black or red circles. Red circles are for the two galaxies B and C, discussed in the text in detail.

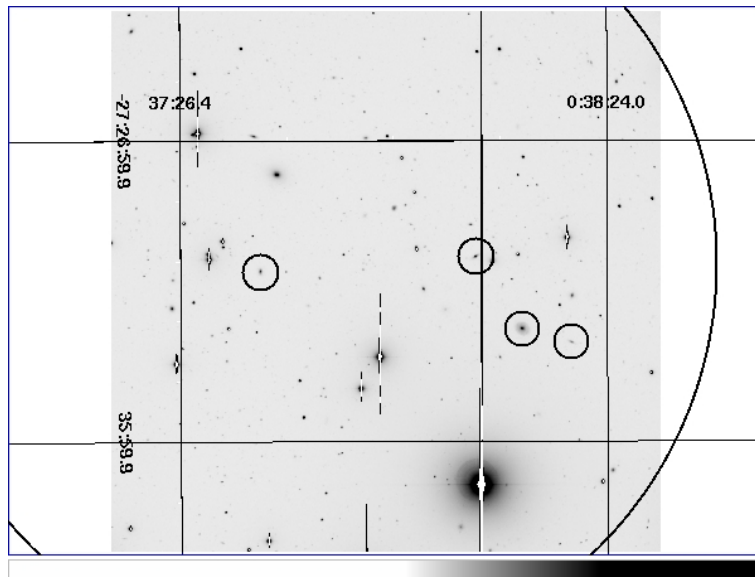


Figure 4.10: The optical image of the group MZ9014. The big black circle, which is partially visible, denotes the GMRT primary beam (FWHM). The small black circles denote the galaxies which could have been detected if they were not H I deficient.